

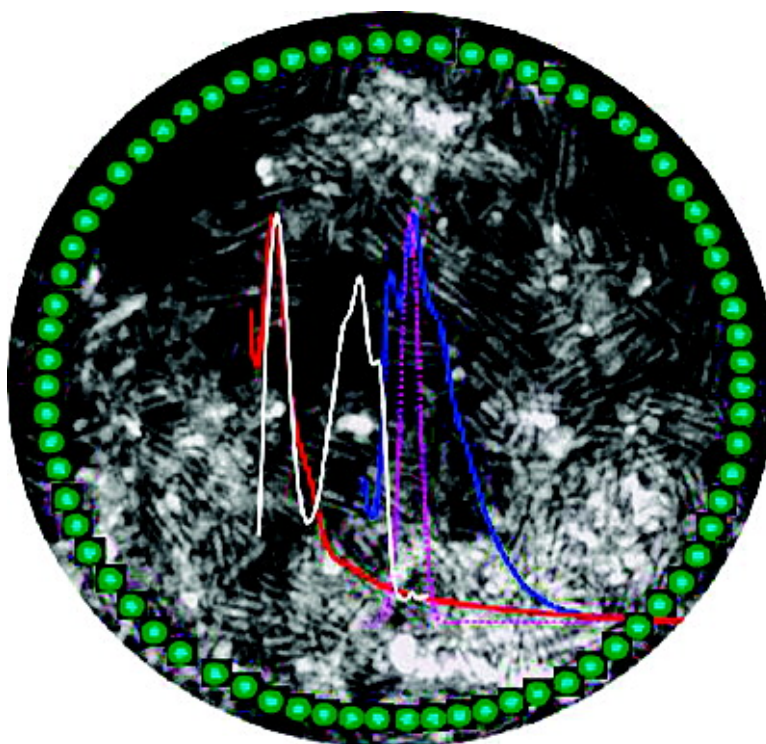
Communication

Ultra Narrow PbS Nanorods with Intense Fluorescence

Somobrata Acharya, Ujjal K. Gautam, Toshio Sasaki, Yoshio Bando, Yuval Golan, and Katsuhiko Ariga

J. Am. Chem. Soc., **2008**, 130 (14), 4594-4595 • DOI: 10.1021/ja711064b

Downloaded from <http://pubs.acs.org> on February 8, 2009



More About This Article

Additional resources and features associated with this article are available within the HTML version:

- Supporting Information
- Access to high resolution figures
- Links to articles and content related to this article
- Copyright permission to reproduce figures and/or text from this article

[View the Full Text HTML](#)



ACS Publications
High quality. High impact.

Ultra Narrow PbS Nanorods with Intense Fluorescence

Somobrata Acharya,^{*,†} Ujjal K. Gautam,[‡] Toshio Sasaki,[†] Yoshio Bando,^{†,‡} Yuval Golan,[¶] and Katsuhiko Ariga[§]

International Center for Young Scientists, Nanoscale Materials Center, and Supermolecules Group, National Institute for Materials Science (NIMS), 1-1 Namiki, Tsukuba 305-0044, Japan, and Department of Materials Engineering and the Ilse Katz Institute for Meso and Nanoscale Science and Technology, Ben-Gurion University, Beer Sheva, Israel 84105

Received December 13, 2007; E-mail: ACHARYA.Somobrata@nims.go.jp

One-dimensional (1D) luminescent semiconductor nanorods and nanowires are of significant interest owing to their potential applications in optoelectronics, nanobiotechnology, and nanoelectronics.¹ Designing ultra narrow nanorods with well-defined shapes and sizes in the strong confinement regime (rod radius, $r \ll$ Bohr radius, a_B) remains a significant challenge in nanotechnology. The necessity for such nanorods of different materials is increasingly growing due to their possible use as nanoscale building blocks for various applications. The interest is particularly true for the IV–VI class of materials which can cover the technologically important wide spectral range from mid-infrared to the visible region, yet have been studied to a lesser extent compared to II–VI semiconductors.² Moreover, their spectral capabilities have not reached the desired confinement level due to unavailability of proper dimension, partially due to difficulties in synthesizing the nanoparticles with well-controlled size and shape at very small scale. Additionally, most of the II–VI and III–V semiconductors have a moderate difference in electron and hole effective masses, leading to significant asymmetry between individual charge carriers and weak confinement for an individual charge carrier.³ In comparison, type IV–VI materials such as lead sulfide (PbS) and lead selenide (PbSe) have large Bohr radii, which allow one to achieve stronger confinement even with relatively larger dimensions.³ From a technological perspective, PbS is an extremely promising material for a large number of applications in the mid- and near-infrared emission and detection range,^{4a} biological applications,^{4b} and optoelectronic devices owing to its wide range of size-dependent properties.^{4c} Recent progress in synthesis now allows fabrication of PbS nanocrystals of a wide variety of shapes and dimensions.⁵ However, comparatively larger sizes of these PbS nanomaterials have restricted the desired levels of quantum confinement. Here we report on uniform, narrowest “free” quantum rods of 1.7 nm in diameter, which allows us the opportunity to test the theories in the strong confinement regime. The strong confinement is reflected in absorption, photoluminescence (PL), and Raman spectroscopy. These rods are strongly fluorescent and display discrete narrow optical spectra with robust stability, which could be useful, for example, in biological labeling, in fluorescence resonance energy transfer (FRET), and in optoelectronics applications.

We have recently reported on the single-step synthesis of ultra narrow nanorods and nanowires by decomposition of single precursor metal xanthate in a suitable ligand.^{6,7} We have extended the synthetic approach to produce ultra narrow PbS rods by decomposition of single precursor lead hexadecylxanthate in a single step in trioctylamine (TOA) as surfactant cum solvent at low

temperature (80 °C, see Supporting Information). Figure 1a and b shows the dark field (DF) transmission electron microscopy (TEM) images of TOA-coated rods of 12–15 nm in length. The control over the aspect ratio can be achieved using the same amount of organometallic precursor injected by increasing temperature (Supporting Information). The bright field high-resolution TEM (HR-TEM) images of individual rods show that the rods are of 1.7 ± 0.2 nm in diameter (Figure 1c) with well-resolved lattice planes corresponding to an interplanar distance of 0.29 ± 0.02 nm, consistent with the (200) d -spacing of the PbS bulk rocksalt structure, and EDS analysis (see Supporting Information) reveals a nearly stoichiometric ratio of Pb to S. The selected area electron diffraction (SAED) patterns of these ultra narrow PbS rods (Figure 1d) confirm the rocksalt cubic structure with predominant 200 and 220 diffraction rings, corresponding to the interplanar distances of 0.2969 and 0.2099 nm of PbS (JCPDS powder diffraction file #05-0592), in line with the interplanar spacings observed in the HRTEM (Figure 1c). The HRTEM image indicates an orientation in which the $\langle 110 \rangle$ crystallographic axis is parallel to the long axis of the rods. The strongest intensity of the 200 reflection is in line with the expected 200/220 intensity ratio of 1:0.57 in the JCPDS powder diffraction file.

The use of amines as capping ligands has been shown to play an important role in determining the nanocrystal shapes and sizes in addition to stabilizing the particles.^{6–8} It is expected that, due to its higher nucleophilic nature, TOA should bind to the lead ions of the inorganic core, at least as strongly as in the case of previously used primary amine capping agents.^{6–8} Notably, the self-assembled 2D supercrystalline pattern similar to Zn-chalcogenide “ordered rods” could not be obtained using TOA as a ligand within the synthetic conditions tested so far.^{6b,8b} The dissimilarity in self-assembly probably originates from differences in the coordination mechanism of the ligands on specific nanocrystal facets, in addition to nucleophilicity of alkyl amines. The faster growth and kinetics of ligand adsorption are markedly different owing to the initial PbS rocksalt facets,^{5c} which is crucial for developing these ultra narrow “random free rods”.

The strong quantum confinement indeed is reflected in the room temperature absorption and PL spectra of the nanorods. The absorption onset (2.84 eV, Figure 2) of the nanorods is strongly blue shifted from the bulk band gap (0.41 eV) and shows discrete sharp excitonic bands at 278 nm (4.47 eV) with a narrow FWHM of ~ 20 nm, a shoulder at 315 nm (3.95 eV) and a weak band at 365 nm (3.41 eV). These bands are of excitonic origin corresponding to $1P_c \leftarrow 1P_h$, $1S_c \leftarrow 1P_h$, and $1S_c \leftarrow 1S_h$ transitions, respectively.⁹ The PL spectrum shows strong and sharp band-edge emissions at 410 and 434 nm, a shoulder at 465 nm, and a weak band at 500 nm, respectively (Figure 2). Deconvolution of the spectrum reveals

[†] International Center for Young Scientist, NIMS.[‡] Nanoscale Materials Center, NIMS.[§] Supermolecules Group, NIMS.[¶] Ben-Gurion University.

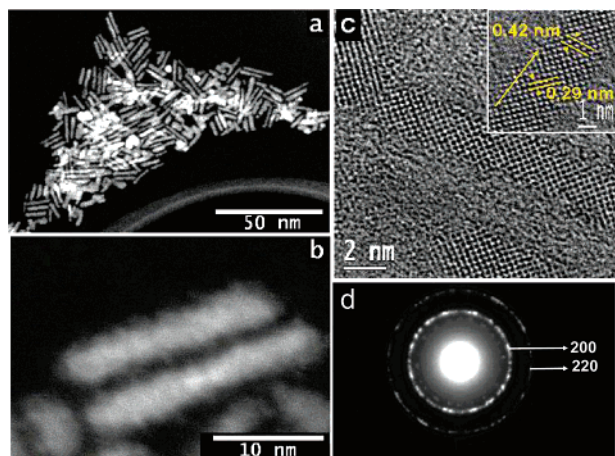


Figure 1. (a, b) Dark field TEM images of ultra narrow PbS rods. (c) HRTEM image of ultra narrow PbS rods showing a diameter of 1.7 nm with well-resolved lattice planes. Inset: HRTEM showing the interplanar distances of the lattice planes; the arrow indicates the growth direction. (d) SAED pattern from the ultra narrow rods.

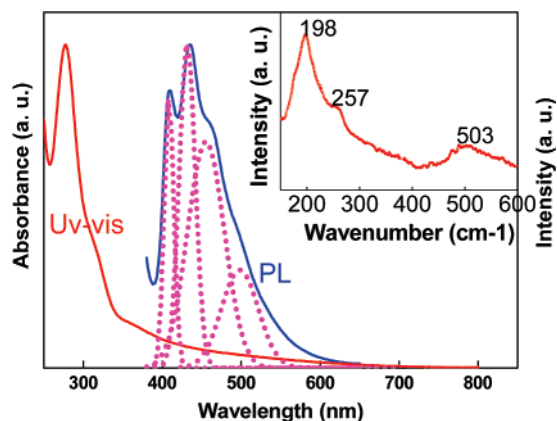


Figure 2. Absorption (red curve) and PL (blue curve; excitation wavelength 350 nm) spectra for 1.7 nm rods in dichloromethane. Deconvolution (magenta dotted curves) shows peaks with narrow widths in PL. Inset: Raman spectra with 644 nm excitation for powder of rods.

very narrow band widths of 112 and 148 meV for the higher energy 410 and 434 nm emissions, respectively. The discrete and sharp optical spectra (characteristic of narrow size distribution) both in UV and PL are blue shifted compared to all previous reports,^{3b,5} suggesting the strongest degree of confinement, as expected in view of the ratio of r to a_B , 0.042 ± 0.005 . Typical quantum yield of the rods measured relative to anthracene dye is 45%. The sharp PL transitions with high quantum yield could be useful in applications such as laser emitters and fluorescence markers. Interestingly, exciton–phonon coupling via Fröhlich interaction of vibrational modes appears at 198 cm^{-1} (angular momentum $lp = 0$) and a reproducible shoulder at $\sim 180 \text{ cm}^{-1}$, corresponding to fourth lowest eigenmode with $lp = 0$, has been observed from the narrow rods (inset of Figure 2).^{9b,c} The shoulder is absent for larger structures (Supporting Information), suggesting lack of surface component modes with $lp \geq 1$ and thus confirming the prediction that the coupled mode frequencies are particle size dependent.^{9c}

Among the variety of methods that exist for spatial organization of nanoparticles, spin casting probably offers the simplest route for solid state assembly. The nanorods formed vortex patterns consisting of micron-sized domains originating from a center of declination on a variety of solid substrates (glass, quartz, mica) upon spin casting (Figure 3a,b). Notably, such patterns cannot be

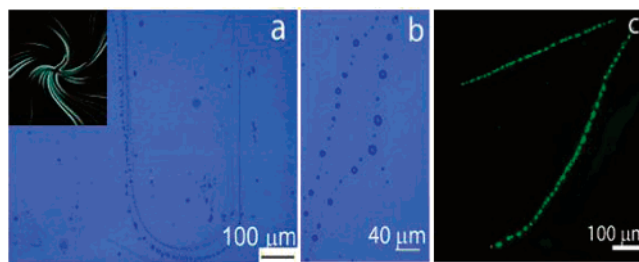


Figure 3. (a, b) Confocal microscopic images of arms of PbS rod vortex at different magnification. The inset of panel a shows a schematic of the nanorod vortex assembly. (c) The ordered domains show fluorescence in the solid state along the vortex arms.

created on a charged surface (e.g., ITO-coated glass, silicon wafer) or with particles of other shapes such as spheres and cubes. This unique pattern formation probably is a result of a delicate balance of the radially outward centrifugal force, frictional forces acting at the interface of the surfactant-coated nanorods and the substrates, and rod dipole^{2a}–surface charge interaction.

One intriguing aspect of this pattern is that the domains which define the pattern can be made discrete or continuous by lowering or raising the suspension concentration. The details of this unique assembly will be addressed separately. Interestingly, the pattern generated fluorescent light (lasts as long as 15 min in air) along its line from the rod domains (Figure 3c), which could be useful in applications such as biological marking. The generality of such assembly opens up new applications in macroscopic pattern formation and new strategies for advanced biological detection, in addition to fundamental physics studies.

Acknowledgment. Financial support from MEXT, Japan Government, is gratefully acknowledged. S.A. gratefully acknowledges I. Patla for preparation of xanthate starting material.

Supporting Information Available: Experimental, size-controlled rods, EDS, Raman spectra. This material is available free of charge via the Internet at <http://pubs.acs.org>.

References

- (1) (a) Duan, X.; Huang, Y.; Agarwal, R.; Lieber, C. M. *Science* **2003**, *421*, 241. (b) Peng, X.; Manna, L.; Wickham, J.; Scher, E.; Kadavanich, A.; Alivisatos, A. P. *Nature* **2000**, *404*, 59. (c) Wang, Z. L.; Song, J. *Science* **2006**, *312*, 242.
- (2) (a) Cho, K.-S.; Talapin, D. V.; Gaschler, W.; Murray, C. B. *J. Am. Chem. Soc.* **2005**, *127*, 7140. (b) Wehenberg, B. L.; Wang, C.; Guyot-Sionnest, P. *J. Phys. Chem. B* **2002**, *106*, 10634.
- (3) (a) Du, H.; Chen, C.; Krishnan, R.; Krauss, T. D.; Harbold, J. M.; Wise, F. W.; Thomas, M. G.; Silcox, J. *Nano Lett.* **2002**, *2*, 1321. (b) Peterson, J. F.; Krauss, T. D. *Nano Lett.* **2006**, *6*, 510.
- (4) (a) McDonald, S. A.; Konstantatos, G.; Zhang, S.; Cyr, P. W.; Klem, E. J. D.; Levina, L.; Sargent, E. H. *Nat. Mater.* **2005**, *4*, 138. (b) Bakueva, L.; Gorelikov, I.; Musikhin, S.; Zhao, X. S.; Sargent, E. H.; Kumacheva, E. *Adv. Mater.* **2004**, *16*, 926. (c) Lu, W.; Fang, J.; Ding, Y.; Wang, Z. L. *J. Phys. Chem. B* **2005**, *109*, 19219.
- (5) (a) Lee, S.; Jun, Y.; Cho, S.; Cheon, J. *J. Am. Chem. Soc.* **2002**, *124*, 11244. (b) Hines, M. A.; Scholes, G. D. *Adv. Mater.* **2003**, *15*, 1844. (c) Lee, S.; Cho, Cheon, S. *J. Adv. Mater.* **2003**, *15*, 441. (d) Shi, W.; Zeng, H.; Sahoo, Y.; Ohulchansky, T. Y.; Ding, Y.; Wang, Z. L.; Swihart, M.; Prasad, P. N. *Nano Lett.* **2006**, *6*, 875.
- (6) (a) Patla, I.; Acharya, S.; Zeiri, L.; Israelachvili, J.; Efrima, S.; Golan, Y. *Nano Lett.* **2007**, *7*, 1459. (b) Panda, A. B.; Acharya, S.; Efrima, S. *Adv. Mater.* **2005**, *17*, 2471.
- (7) (a) Acharya, S.; Patla, I.; Kost, J.; Efrima, S.; Golan, Y. *J. Am. Chem. Soc.* **2006**, *128*, 9294. (b) Acharya, S.; Panda, A. B.; Efrima, S.; Golan, Y. *Adv. Mater.* **2007**, *19*, 1105.
- (8) (a) Mokari, T.; Zhang, M.; Yang, P. *J. Am. Chem. Soc.* **2007**, *129*, 9864. (b) Pradhan, N.; Efrima, S. *J. Phys. Chem. B* **2004**, *108*, 11964.
- (9) (a) Machol, J. L.; Wise, F. W.; Patel, R. C.; Tanner, D. B. *Phys. Rev. B* **1993**, *48*, 2819. (b) Krauss, T. D.; Wise, F. W. *Phys. Rev. B* **1997**, *55*, 9860. (c) Krauss, T. D.; Wise, F. W.; Tanner, D. B. *Phys. Rev. Lett.* **1996**, *76*, 1376.

JA711064B